A multispectral tunnel inspection system for simultaneous moisture and shape detection

Valentin Vierhub-Lorenz*[a], Katharina Predehl[a], Sebastian Wolf[a], Christoph S. Werner[a], Frank Kühnemann[a], Alexander Reiterer[a,b]

[a] Fraunhofer Institute for Physical Measurement Techniques IPM, Freiburg, Germany;
[b]Albert-Ludwigs-University Freiburg, Chair Monitoring of Large-Scale Structures INATECH, Freiburg, Germany

ABSTRACT

In this paper, we present the implementation of a differential-absorption measurement-technique for surface moisture detection into a laser scanner aiding modern tunnel inspections. The use of laser scanners for tunnel inspections can reduce costly tunnel closures and provide digital data, compliant with modern building information modeling (BIM). Unfortunately, available systems are typically limited to pure 3D mapping. The Fraunhofer Institute for Physical Measurement Techniques IPM is developing a novel multi-parameter laser scanning system. For the first time, this system allows the simultaneous measurement of 3D-geometry, remission and surface moisture. The scanner measures simultaneously with two collinear laser beams with distinct wavelengths. One is centered at the absorption band of water at 1450 nm wavelength, while the other, with 1320 nm wavelength, is used as an intensity reference. The intensity ratio gives a good estimate of the surface water content. Additionally, the power of both lasers is modulated with a high frequency. This enables simultaneous measurement of the distance by comparing the phase difference of the backscattered light with a local reference. With this approach, we are able to record up to two million points per second containing distance, intensity and moisture information. Besides the technical implementation, we present point clouds from multiple test objects and surfaces. The presented data nicely demonstrates the ability to differentiate between absolute intensity variations, e.g. caused by dirt, and actual water contamination.

Keywords: Tunnel inspection, surface moisture, water leakage, multispectral, differential absorption, laser scanner

1. INTRODUCTION

Tunnels, as a crucial part of transport infrastructure, require regular inspections and maintenance to ensure structural stability and a safe operation [1]. Typically, these inspections comprise the precise measurement of the tunnel geometry as well as the detection of cracks and moisture in the tunnel linings. Changes in the tunnel geometry compared to previous inspections indicate deformations and give insight to whether a tunnel needs reinforcement. Cracks, as well as water inrush, can indicate deeper structural damages and need to be documented thoroughly. Moisture can further lead to structural damages, e.g. the corrosion of steel, the degradation of mortar due to dissolved salts, frost damages or the growth of organic material [2,3,4]. Still, these inspections are labor-intensive and time-consuming tasks conducted mostly visually and by the use of tactile measurement instruments. The results are incomplete datasets, poor documentation and subjective assessment. Over the last decade, laser scanners became a valuable tool for modern tunnel inspections. Mounted on a vehicle, they generate comprehensive data on the remission and 3D-geometry in a single drive through, making longer tunnel closures obsolete. The digital data is consistent with the more and more important building information modeling and easily allows to detect deviations by direct comparison with data from previous inspections. For the automatic and thorough detection of surface moisture, different methods are used. In Ref. 5 the use of the intensity values of a laser scanner to detect wet spots is proposed, in Ref. 6 they use infrared thermography to obtain information about the surface temperature and from that extrapolate wet spots. Both techniques hold disadvantages when it comes to the misjudgment of wet areas as they only evaluate an unbalanced intensity or temperature value.

*valentin.vierhub-lorenz@ipm.fraunhofer.de; phone +49 761 8857-283; www.fraunhofer.ipm.de

However, a tunnel-surface remission-change can have various other reasons such as dirt stains, material changes or similar, resulting in a poor significance of such measurements. The same is true for colder spots on the tunnel surface, which are not necessarily linked to water. In Ref. 7 a combination of thermal imaging with laser scanning data is proposed and the authors could show that it is possible to increase the detection accuracy in some special situations. Still, the major drawbacks persist: The method needs multiple instruments and features a weak selectivity. In this paper, we present the implementation of differential-absorption measurement-technique in the near infrared (NIR) spectral region that allows the integration of surface moisture detection into a laser scanner. This allows a reliable detection of surface moisture in conjunction with the generation of an accurate 3D-point cloud and will be another step towards fully automated tunnel inspections.

2. MOISTURE DETECTION BY NIR-ABSORPTION MEASUREMENT

2.1 Absorption Spectrum of Water in the NIR region

Water shows distinct absorption lines in the NIR spectral region that originate from the excitation of vibration and rotation states of the molecule. Opposed to the sharp absorption lines of gaseous water vapor, for liquid water the lines are affected by hydrogen bonding and appear as broad absorption bands. Figure 1a) shows the liquid water absorption spectrum between 1 µm and 2 µm wavelength. Exploiting this distinctive water absorption spectrum is already common practice in various fields such as moisture content monitoring in food [8,9]. In addition, Hemmleb et al. proposed this method to detect moisture on the surface of construction materials [10]. Our goal was to implement this technique into a laser scanner to obtain a 3D-model of the structure of interest, which also shows the surface moisture content. In the resulting point cloud, one can easily locate wet areas, e.g. caused by leakages. In a first step, the spectra of plaster in different moisture conditions have been measured by illuminating a sample with a supercontinuum laser source with a spectral range from approximately 500 nm to 2400 nm and analyzing the scattered intensity with a line spectrometer (Ocean Optics NIR-Quest). The results are shown in Fig. 1b). The spectra are normalized to the diffuse reflection of a reference target made of a gold coated, sand blasted surface. The two absorption bands at approximately 1450 nm and 1920 nm wavelength become more dominant the higher the moisture content of the plaster. One can also observe an overall reduction in remission with increasing moisture. This is a visualization of the effect that objects typically appear darker to us when they are wet. The phenomenon mainly originates from total internal reflection on the water-air surface as described in Ref. 11 and increased forward scattering into the wet material as described in Ref. 12. Depending on the surface properties such as roughness and particle size, one or the other contribution is more dominant.

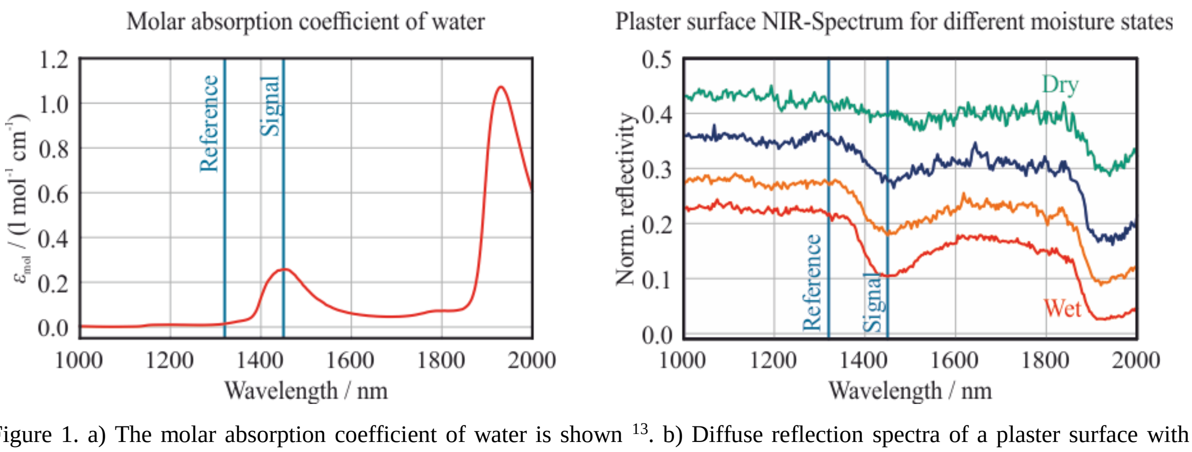

Figure 1. a) The molar absorption coefficient of water is shown [13]. b) Diffuse reflection spectra of a plaster surface with increasing surface moisture. The spectra are normalized to the reflected signal of a diffusive gold surface. The green curve shows the diffuse reflection for a dry plaster surface, which was stored at room temperature at approximately 30% relative humidity. From blue over orange to red the water content is increased where for the red curve the plaster was saturated with water with some excess water on the surface. The two blue lines in both graphs indicate the wavelengths at 1320 nm and 1450 nm that we are using in our laser scanner to detect moisture.

2.2 Using differential absorption to detect moisture

By simultaneously illuminating a target with two light waves, one with a wavelength centered in an absorption band of water and a reference wave which is unaffected by the absorption band, from the measured backscattered light one can calculate a coefficient which correlates with the amount of water on the target surface. We chose 1450 nm as the first wavelength, which gets absorbed by water and 1320 nm as the reference wavelength. Even though water exhibits even stronger absorption at 1920 nm, the availability of cost-effective diode lasers at 1450 nm made us go for this wavelength. The reference wavelength is chosen to be close to 1450 nm without being affected by the absorption band itself. This reduces the effect of chromatic aberration in our collinear optical setup and allows us the neglection of a wavelength dependence in the surface's scattering properties. A unit less moisture value M is then given by

$$M = \frac{I_{\mathrm{ref}} - I_{\mathrm{abs}}}{I_{\mathrm{ref}}}. \tag{1}$$

Here, I_{ref} denotes the backscattered intensity at the reference wavelength of 1320 nm and I_{abs} the backscattered intensity at the wavelength of 1450 nm, which is centered at the absorption band of water. Both intensities are individually normalized to the backscattered intensity of a dry target with a near lambertian scattering behavior and approximately 90% reflectivity. The so obtained moisture value can be used to distinguish between actual leakages and wet spots on a surface and a reduction in overall intensity caused from material changes, paint, dirt, etc. One has to note that so far this value only gives an estimation on the moisture state, i.e. a relative moisture, of the surface but not an absolute amount of water content of the examined material. This is strongly material and surface texture dependent. If the absolute value is required, additional prior knowledge of the examined material and a calibration curve obtained by a reference measurement is needed.

3. MULTIWAVELENGTH SENSOR SYSTEM FOR TUNNEL INSPECTIONS

The presented laser scanner is based on the phase measurement ranging technique. Here, the intensity of a continuous wave laser is modulated with a frequency typically between 1 MHz and 1 GHz. The phase between a local oscillator and the backscattered intensity is compared. Via Eq. 2 the distance D to the object can be calculated by the measured phase difference $\Delta\theta$, the modulation frequency f and the speed of light c.

$$D = \frac{\Delta\theta\ c}{4\pi\ f} + \frac{n\ c}{2\ f} \tag{2}$$

The phase difference can only be measured from 0 to 2π and then repeats itself, limiting the unambiguity range. The arbitrary positive integer n stands for the multiple of 2π that the phase difference has exceeded and cannot be measured. Therefore, the modulation frequency has to be chosen such that the desired measurement region does not exceed a 2π phase difference. In our case, the setup consists of two fiber coupled laser diodes, emitting at 1450 nm and 1320 nm wavelength respectively. The optical output power is modulated with 128 MHz and 8 MHz for the 1450 nm laser and 96 MHz and 6 MHz for the 1320 nm laser. The lower frequencies are used for a less precise estimate of the absolute distance but with a large unambiguity of 18.75 m for the 8 MHz modulation frequency. The higher frequencies provide a precise distance estimation within the unambiguity range of the lower frequencies. The modulation ratio between the low and the high frequencies is approximately 50/50 and the overall modulation depth is around 85%. Via a wavelength division multiplexer, the two laser beams are joined into one single mode fiber. The collinear beams exit the fiber through a collimator and are deflected by a small mirror through a hole in the center of the receiving optics. The result is a coaxial alignment of the illuminating beam and the receiving light path. A rotating polygon deflects the beam along a scan-line. The backscattered light from the target is focused on an InGaAs avalanche photodiode (APD). An important aspect of the design is the use of a single detector for both waves. As both waves possess individual modulation frequencies, their individual contribution can be reconstructed in the subsequent signal processing: Through electronic filtering and mixing with a local oscillator the four contributions are separated and their phase difference relative to that of the local oscillator as well as their amplitudes are determined. From the phase differences we obtain the target distance as described earlier and the amplitudes are used to calculate the remission and moisture value as described in chapter 2.2. With this measurement technique, we achieve up to 2 million single measurements per second. For concrete, the moisture values typically range from 0 in dry state to 0.5 in wet state with some excess water on the surface. The values show an uncertainty of $\sigma = \pm 0.05$ for a target at a distance of 5 m and a reflectivity of 90%. This measurement uncertainty is dominated by speckle-induced noise.

The system scans only along a single line, in a typical mobile mapping scenario, the movement of a vehicle allows a two-dimensional measurement as the scanner is mounted perpendicular to the driving direction. By using an inertial measurement unit (IMU) and either a global positioning system (GPS) or reference marks one can get the trajectory and from that calculate the georeferenced 3D-point cloud. In our prototype, we mimic this by a motorized stage turning the setup with a known angular velocity.

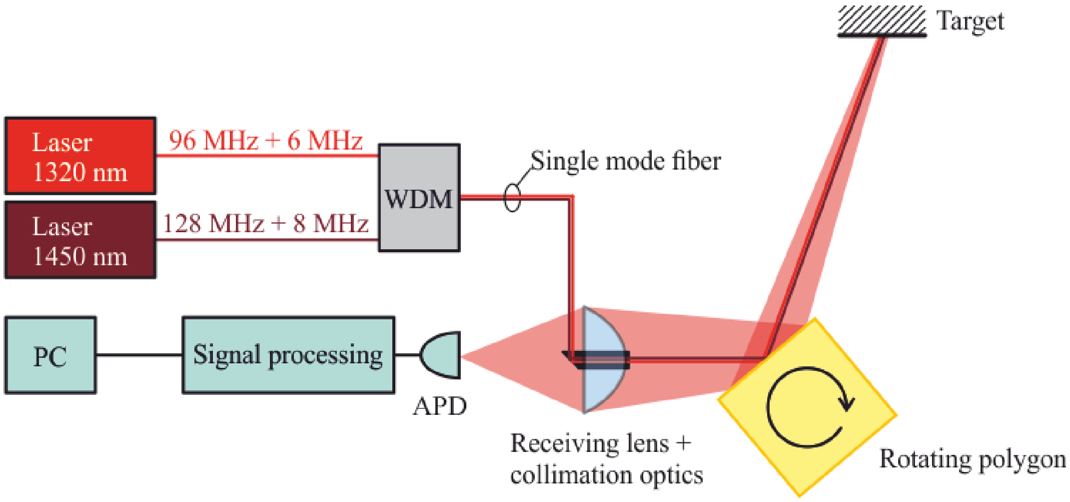

Figure 2. Schematic depiction of the sensor system. Two fiber-coupled lasers with wavelengths of 1320 nm and 1450 nm are modulated, each by two frequencies. The light is combined by a wavelength division multiplexer (WDM), collimated and deflected by a small mirror through a hole in the center of the receiving lens to form a coaxial beam path with the backscattered light. A rotating polygon deflects the beam. The backscattered light is focused on an avalanche photodiode (APD). The generated current is analyzed by signal processing electronics and the phase differences are calculated. A computer (PC) generates a point cloud from the obtained signals, the encoder values of the polygon and the data about the trajectory the scanner has moved.

4. RESULTS

With the setup described in section 3 several test measurements have been performed. To confirm and evaluate the capability of the system five concrete blocks with different moisture states and overall reflectivity have been scanned. Fig. 3 shows a photograph of the scanned scenario as well as false-colour representations of the measured intensity and moisture values. The blocks on the bottom have untreated surfaces whereas the top ones are spray-painted with black paint to appear darker. The blocks on the left hand side are very moist. They have been submerged in water for at least 30 min prior to the experiment. The middle blocks have been sprayed with water using a hand-held spry gun. The dry blocks on the left hand side have been stored at room temperature and 30% relative humidity for over 24 hours. In the point cloud, which is colored only with the intensity value of the reference laser, one cannot distinguish a wet concrete block from one with an overall reduced reflectivity. The scan that is color-coded using the calculated moisture value clearly shows the different states of moisture without noticeable influence of the reflectivity of the target.

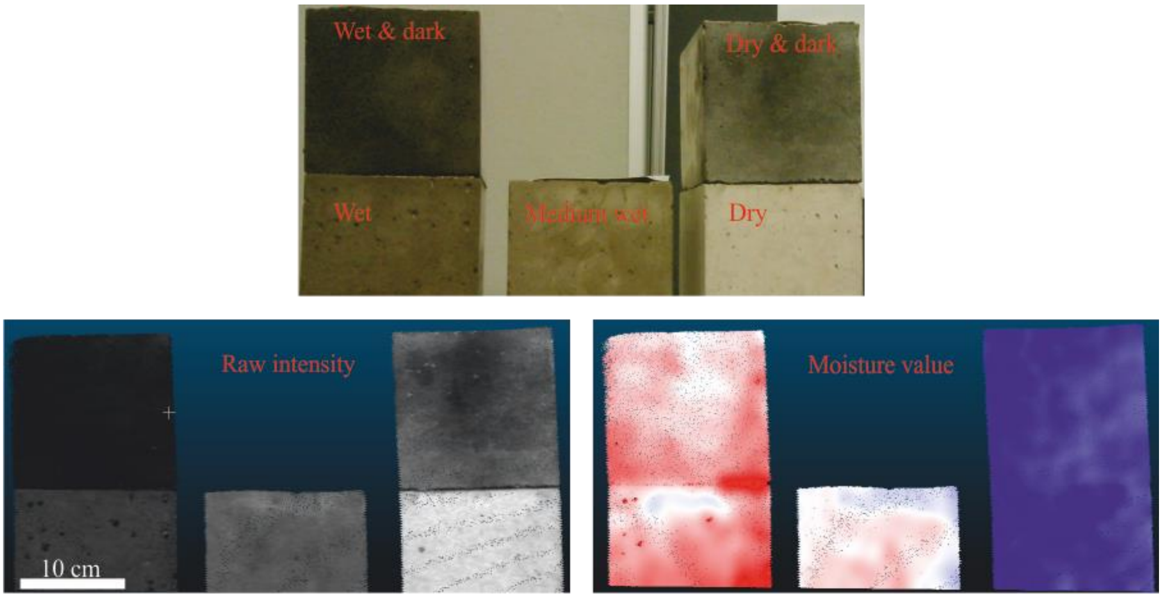

Figure 3. Top: A photograph of the five investigated concrete blocks. The size of one block is 15 cm x 15 cm. The two blocks on the top have been sprayed with black paint to appear darker and simulate dirt. The moisture state of the blocks changes from saturated wet with some excess water on the surface for the left blocks over moist for the block in the middle to dried at room temperature and approximately 30% relative humidity for the right blocks. Lower left: The image shows a scan obtained with the in section 3 described setup and colored using only intensity values. It is not possible to distinguish whether a block is just darker or actually wet. Lower right: The image shows the same scan but colored using the moisture value. The moisture values M range from around 0 for dark blue (dry surfaces) to almost 0.5 for red (wet areas). A Gaussian filter with a 5 mm sigma has been applied to reduce noise. The moisture states are clearly visible.

Furthermore, an ensemble of different materials was scanned in both dry and wet state in order to investigate the dependency of the measured moisture value of the substrate. The ensemble as well as the scans colored with the moisture value are shown in Fig. 4. The difference between wet and dry state becomes clearly visible for all materials. The values for the dry state are around 0 for all materials with slight deviations of around ±0.05. The values for the wet state vary more which we attribute mainly to the different capabilities to absorb water.

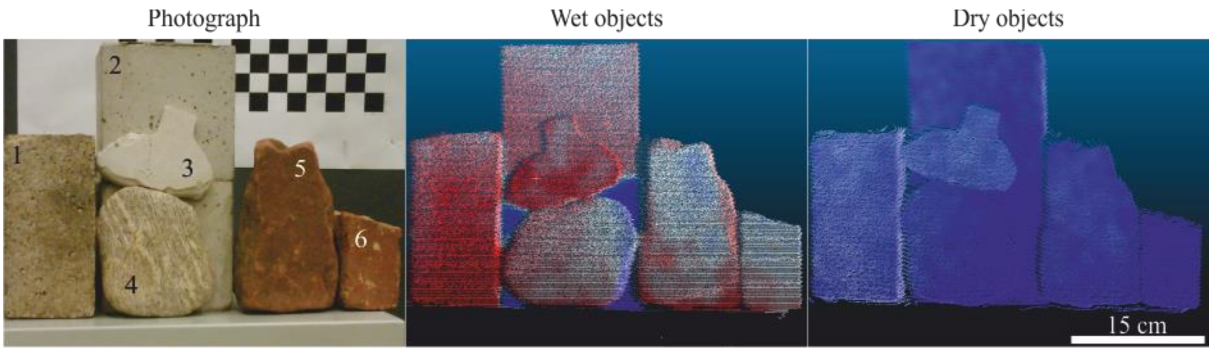

Figure 4. Left: A photograph of various construction materials that have been scanned in wet and dry surface moisture state. The ensemble from left to right consists of a coarse concrete stone (1), a piece of plaster (3) in front of two smooth concrete blocks (2), a natural stone (4) and a red sandstone (5) and a brick (6). In the middle and on the right two scans that are colored using the moisture value are shown, in wet and dry state of the samples. The moisture values M range from around 0 for dark blue (dry surfaces) to almost 0.5 for red (wet areas). A Gaussian filter with a sigma of 5 mm has been applied to the moisture values to reduce noise.

Finally, the system was tested in a realistic setting on a construction site, where several concrete and plaster surfaces have been scanned. Parts of the surfaces have been sprayed with water. A photograph of the prototype in front of a scanned scenery as well as the resulting point cloud is shown in Fig. 5. The wet spots have a good contrast from the dry surroundings. A differentiation between wet spots and dark stains on the concrete column on the right is easily possible. In the scan, one can observe spurious horizontal changes in the moisture value of the dry surfaces. They originate from a varying detection ratio between the two wavelengths depending on the distance of the target. A solution to this problem is a distance depending normalization factor for both of the measured amplitudes, obtained by a calibration measurement, which has not been conducted for this prototype.

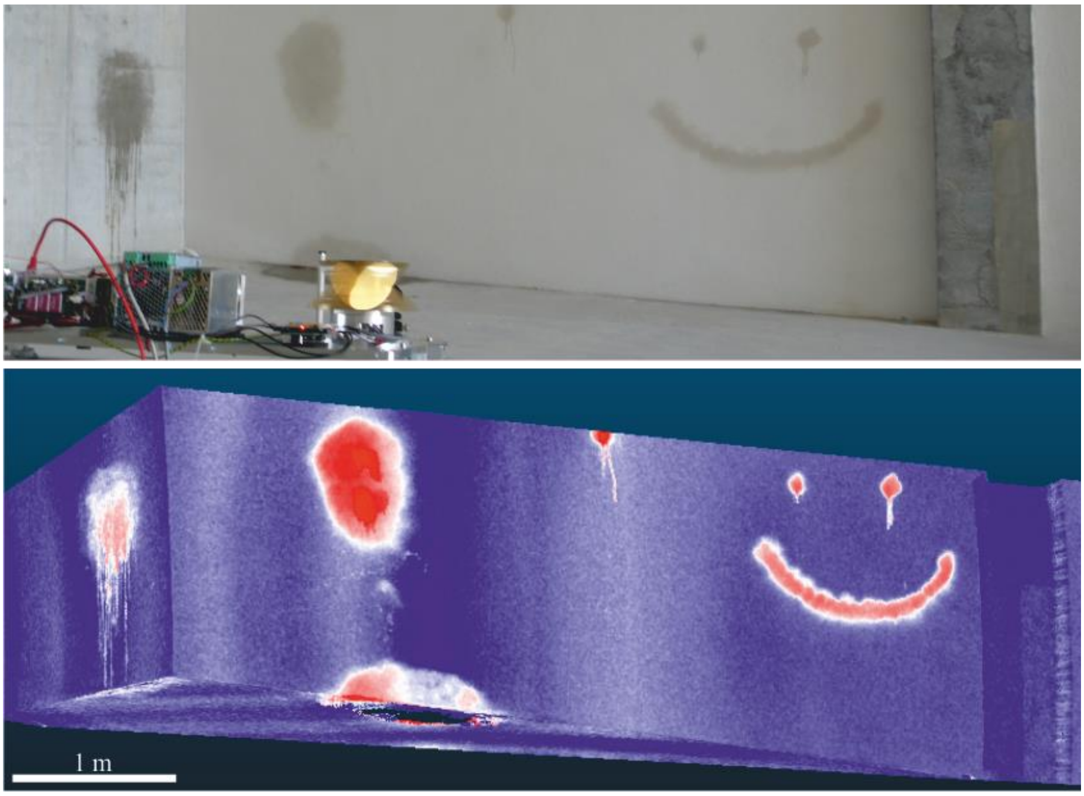

Figure 5. Top: Photograph of the prototype in front of a scanned scenery of concrete and plaster surfaces with wet spots. Bottom: Scan of the scenery, colored using the moisture value. The wet spots have a good contrast to the dry surroundings. The moisture values M range from around 0 for dark blue (dry surfaces) to almost 0.5 for red (wet areas). A Gaussian filter with a sigma of 5 mm has been applied to the moisture values to reduce noise.

5. CONCLUSION

We present a novel sensor system for modern tunnel inspection. The system allows the simultaneous measurement of the 3D-geometry, surface reflectivity and surface moisture of tunnel structures. The surface moisture values are derived from dual-wavelength differential absorption measurements in backscattering geometry. A demonstration of the technique is given by a rapidly line scanning system on a swivel mount to allow for 3D mapping of test scenarios. Data sets can be recorded at an acquisition rate of 2 MHz. Test measurements demonstrate the ability to differentiate between wet and dry surfaces of various construction materials in a 3D-point cloud. So far, the system consists of a laboratory setup with one detector. Further development of the system will include additional measurement channels in order to form a prototype with a 360° field of view. The high measurement rate of at least six million points per second for a 360° scan will allow a fast and thorough measurement of the whole tunnel surface without costly tunnel closures. In the near future, the system will be tested in actual tunnels under real conditions.

REFERENCES

[1] Deutsches Institut für Normung, "Ingenieurbauwerke im Zuge von Straßen und Wegen: Überwachung und Prüfung," DIN: 1076, (1999).

[2] ITA Working Group on Maintenance and Repair of Underground Structures, "Report on the damaging effects of water on tunnels during their working life," Tunn. Undergr. Sp. Tech. 6, 11-76 (1991).

[3] Balak, M. and Pech, A., [Mauerwerkstrockenlegung: Von den Grundlagen zur praktischen Anwendung], Springer, Wien, (2003).

[4] Rauch, P., [Tauwasser und Feuchtigkeit im Mauerwerk], Ingenieurbüro Peter Rauch, Leipzig, (2011).

[5] Xu, T., Xu, L., Li, X. and Yao, J., "Detection of water leakage in underground tunnels using corrected intensity data and 3D point cloud of terrestrial laser scanning," IEEE Access 6, 32471-32480 (2018).

[6] Grinzato, E., Ludwig, N., Cadelano, G., Bertucci, M., Gargano, M. and Bison, P., "Infrared thermography for moisture detection: A laboratory study and in-situ test," Materials Evaluation 69 (2011).

[7] Yu, P., Wu, H., Liu, C. and Xu, Z., "Water leakage diagnosis in metro tunnels by intergration of laser point cloud and infrared thermal imaging," ISPRS XLII-3. 2167-2171 (2018).

[8] Büning-Pfaue, H., "Analysis of water in food by near infrared spectroscopy," Food Chem. 82(1), 107-115 (2003).

[9] Lin, L., He, L., Xiao, Z., Zhao, K., Dong, T. and Nie, P., "Rapid-detection sensor for rice grain moisture based on NIR spectroscopy," Appl. Sci. 9(8) (2019).

[10] Hemmleb, M., Weritz, F., Schiemenz, A., Grote, A., Maierhofer, C., "Multispectral data acquisition and processing techniques for damage detection on building surfaces," Proc. ISPRS Commission V Symposium XXXVI (2006).

[11] Lekner, J. and Dorf, M. C., "Why some things are darker when wet," Appl. Optics 27 (1988).

[12] Twomey, S. A., Bohren, C. F. and Mergenthaler, J. L., "Reflectance and albedo differences between wet and dry surfaces," Appl. Optics 25 (1986).

[13] Bertie, J. E. and Lan, Z., "Infrared intensities of liquids XX: The intensity of the OH stretching band of liquid water revisited, and the best current values of the optical constants of $H_2O(l)$ at 25°C between 15,000 and 1 cm^{-1}," Appl. Spectrosc. 50(8), 1047-1057 (1996).